Controlling the Charge State and Redox Properties of Supported Polyoxometalates via Soft Landing of Mass-Selected Ions

ARTICLE *in* THE JOURNAL OF PHYSICAL CHEMISTRY C · DECEMBER 2014

Impact Factor: 4.77 · DOI: 10.1021/jp505050m

8 AUTHORS, INCLUDING:

Grant Johnson
Pacific Northwest National Laboratory
44 PUBLICATIONS **987** CITATIONS
SEE PROFILE

Weiying Zhang
JiangHan University
14 PUBLICATIONS **192** CITATIONS
SEE PROFILE

Venkateshkumar Prabhakaran
Pacific Northwest National Laboratory
17 PUBLICATIONS **158** CITATIONS
SEE PROFILE

Yuehe Lin
Washington State University
363 PUBLICATIONS **21,260** CITATIONS
SEE PROFILE

THE JOURNAL OF PHYSICAL CHEMISTRY C

Article

pubs.acs.org/JPCC

Controlling the Charge State and Redox Properties of Supported Polyoxometalates via Soft Landing of Mass-Selected Ions

K. Don D. Gunaratne, Grant E. Johnson, Amity Andersen, Dan Du, Weiying Zhang, Venkateshkumar Prabhakaran, Yuehe Lin,† and Julia Laskin*

Pacific Northwest National Laboratory, Physical Sciences Division, P.O. Box 999, MSIN K8-88, Richland, Washington 99352, United States

Supporting Information

ABSTRACT: We investigate the controlled deposition of Keggin polyoxometalate (POM) anions, $PMo_{12}O_{40}^{3-}$ and $PMo_{12}O_{40}^{2-}$, onto different self-assembled monolayer (SAM) surfaces via soft landing of mass-selected ions. Utilizing in situ infrared reflection absorption spectroscopy (IRRAS), ex situ cyclic voltammetry (CV), and electronic structure calculations, we examine the structure and charge retention of supported multiply charged POM anions and characterize the redox properties of the modified surfaces. SAMs of alkylthiol (HSAM), perfluorinated alkylthiol (FSAM), and alkylthiol terminated with NH_3^+ functional groups (NH_3^+SAM) are chosen as model substrates for soft landing to examine the factors that influence the immobilization and charge retention of multiply charged anionic molecules. The distribution of charge states of POMs on different SAM surfaces is determined by comparing the IRRAS spectra with vibrational spectra calculated using density functional theory. In contrast with the results obtained previously for multiply charged cations, soft-landed anions are found to retain charge on all three SAM surfaces. This charge retention is attributed to the substantial electron binding energy of the POM anions. Investigation of redox properties by CV reveals that while surfaces prepared by soft landing exhibit similar features to those prepared by adsorption of POM from solution, the soft-landed POM^{2-} has a pronounced shift in oxidation potential compared with POM^{3-} for one of the redox couples. These results demonstrate that ion soft landing is uniquely suited for precisely controlled preparation of substrates with specific electronic and chemical properties that cannot be achieved using conventional deposition techniques.

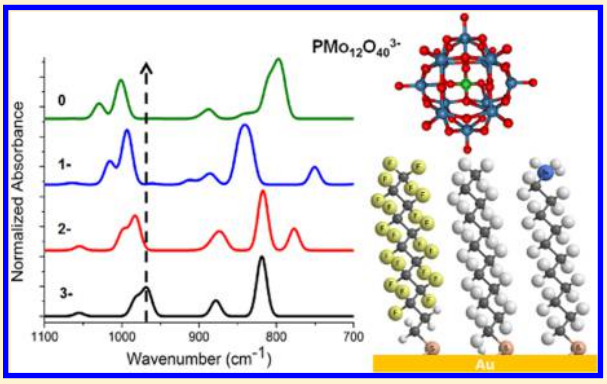

INTRODUCTION

Precise control of the charge state of supported molecules is important for tailoring the chemical, electronic, and magnetic properties of functionalized surfaces that are of interest for applications such as catalysis and molecular electronics.[1−4] Control over the charge state of atoms and molecules on surfaces has been achieved experimentally[2−9] and examined theoretically.[10,11] For example, the charging/discharging of nanoparticles on substrates for use as efficient nanoscale memory devices,[12,13] selective adsorption of CO and NH_3 by mass-selected molybdenum sulfide cations on gold surfaces,[14] as well as the improved catalytic activity toward the oxidation of adsorbed CO molecules by partially charged gold clusters on metal oxide supports[1,15] illustrate the wide range of possibilities. These studies revealed that the overall charging characteristics of surfaces may be tuned by the appropriate choice of adsorbed atoms/molecules and substrate. Furthermore, gas-phase studies of metal oxide cluster ions have demonstrated the influence of charge state on the activity and selectivity of chemical reactions of interest to heterogeneous catalysis.[16−19] However, to the best of our knowledge, the properties of intact, charge-selected, multiply charged metal oxide anions deposited onto well-defined substrates have not been characterized thus far. Here we present a study of the properties of charge-selected polyoxometalate (POM) anions deposited on different self-assembled monolayer (SAM) surfaces using ion soft landing.

Ion soft landing enables the deposition of uniform films of intact mass-selected polyatomic ions, in well-defined charge states, from the gas phase onto surfaces.[20−25] This capability provides a unique opportunity to study the ions of interest in the absence of interference from impurities, solvent molecules, and counterions that are inherently present on surfaces prepared using conventional deposition methods. In addition, the ions are deposited onto a well-defined area without agglomeration, as is commonly observed in direct deposition from solution.[26] As a result, this technique is capable of producing the highest possible density of isolated charged clusters dispersed uniformly on a surface. Ion soft landing has established itself as a powerful preparatory mass spectrometric technique[21−25] and may prove to be a valuable approach for the

Received: May 22, 2014
Revised: September 30, 2014
Published: October 7, 2014

   dx.doi.org/10.1021/jp505050m | J. Phys. Chem. C 2014, 118, 27611−27622

controlled fabrication of well-defined POM-based interfaces, complementary to the current methods used for producing such systems.[27]

Evidence of charge retention by soft-landed ions was initially observed in a seminal study by Cooks et al.,[28] where intact organic cations were detected on a SAM of perfluorinated alkylthiol (FSAM). In previous studies of native cations that are inherently charged and are not ionized by attachment of a separate cation or proton, we found that the 3+ charge state of deposited gold clusters was retained on the FSAM surface up to a certain coverage, while alkylthiol SAMs terminated with a carboxyl group (COOH-SAM) and methyl group (HSAM) predominately retained the clusters in the 2+ and 1+ charge states, respectively.[29,30] It was suggested that on HSAM surfaces the deposited cations underwent almost instantaneous neutralization through electron transfer from the underlying metal surface,[30] while the ions deposited on FSAMs exhibited a very slow charge reduction. This charge retention on FSAM is attributed to the large barrier for electron transport introduced by the high electronegativity of fluorine, which withdraws electron density from the alkyl chains of the monolayer while simultaneously inducing an interface dipole at the metal−organic boundary.[31,32] Several other studies examined the behavior of positive ions on surfaces,[33−41] while little is currently known about the charge retention, reduction, and neutralization of negative ions. In this study, we investigate these processes using multiply charged POM anions as a model system.

The well-known ability of POMs to undergo rapid, reversible oxidation−reduction reactions while maintaining their primary structures[42−46] makes them attractive systems for potential applications in electrochemical supercapacitors,[43] batteries,[47] catalysts,[48] drug delivery,[49,50] photochromic devices,[46,51] and microelectronics.[52,53] We focus on Keggin POMs $[PMo_{12}O_{40}]^{3-}$ because they are particularly well-characterized[54−58] and are of interest for a range of applications.[59,60] Although the majority of POM-based applications involve deposition of POMs onto supports, the effect of the surface interaction on the physical and chemical properties of the supported POMs is currently poorly understood.

Here we present an investigation of the structure and redox properties of different charge states of multiply charged anionic POMs soft-landed onto three different SAM surfaces utilizing a combination of in situ IRRAS, electronic structure calculations, and ex situ electrochemical methods. The FSAM and HSAM surfaces were chosen as relatively inert substrates, which are known to have different electron transfer properties.[28,29,61] The NH_3^+SAM was chosen because it has a positively charged terminal functional group that has been shown previously to bind anionic POMs through strong electrostatic interactions.[62] A detailed characterization of the POM−SAM interactions was facilitated by comparing the experimental in situ IRRAS spectra with spectra calculated using DFT. Remarkably, we observed that the POM anions soft-landed on HSAM and NH_3^+SAM exhibit charge retention comparable to that found on the FSAM surface. We find that the charge retention of POMs is primarily determined by the electron binding energy of the deposited anions, while the influence of terminal functional groups and electronic properties of the SAM surfaces are of secondary importance. Ex situ electrochemical analysis demonstrated that while POM anions soft-landed onto the NH_3^+SAM have similar redox properties to POMs adsorbed from solution, one of the redox processes is affected by the charge state of the anion. Our results demonstrate that soft landing of charge- and mass-selected ions may be used to control the charge-state and redox properties of this important class of negatively charged metal-oxide molecules on surfaces.

EXPERIMENTAL SECTION

Chemicals. Sodium phosphomolybdate hydrate ($Na_3[PMo_{12}O_{40}]\cdot xH_2O$ CAS: 1313-30-0), phosphomolybdic acid hydrate ($H_3[PMo_{12}O_{40}]\cdot xH_2O$ CAS:51429-74-4), 1-dodecanethiol (HSAM), 1*H*,1*H*,2*H*,2*H*-perfluorodecanethiol (FSAM), and 11-amino-1-undecanethiol hydrochloride (NH_2SAM) were purchased from Sigma-Aldrich and used as received.

Preparation of Self-Assembled Monolayer Surfaces on Gold. The HSAM,[63] FSAM,[64] and NH_3^+SAM[65] surfaces were prepared following literature procedures. The NH_3^+SAMs were obtained by sonication of NH_2SAM surfaces in a solution of 10% v/v acetic acid in ethanol. All SAMs were prepared on 10 × 10 mm polycrystalline gold surfaces purchased from Platypus Technologies (Madison, WI) with a 50 Å Ti adhesion layer and 1000 Å Au layer on a Si wafer. The gold surfaces were sonicated in ethanol for 10 min, dried using N_2 gas, and cleaned in an ultraviolet/ozone cleaner for 20 min before immersing in 1 mM ethanolic solutions of the respective thiols for at least 24 h. The substrates were then rinsed with ethanol and sonicated in fresh ethanol for 5 min to remove any loosely bound secondary thiols. The NH_2SAMs were rinsed and sonicated with 10% v/v acetic acid in ethanol to ensure protonation of the terminal amine groups. All surfaces were rinsed with ethanol again, dried under N_2 gas, and placed in vacuum for deposition of POMs.

Soft Landing of Polyoxometalates onto SAMs. Soft-landing experiments were conducted using an ion deposition apparatus coupled to in situ IRRAS described in detail previously.[66,67] The negative POM ions were produced from solution (100 μM in methanol) via electrospray ionization[68] (ESI) and introduced into the vacuum system using a heated stainless-steel capillary and an electrodynamic ion funnel.[69] The ions were then thermally relaxed and collimated by collisions with the background gas in an RF-only quadrupole (CQ) maintained at a pressure of 2×10^{-2} Torr and subsequently mass-selected using a resolving quadrupole mass filter (Extrel, Pittsburgh, PA) maintained at 8×10^{-5} Torr during ion deposition. The mass-selected ions were then refocused with three einzel lenses in series before being soft-landed on the SAM surfaces. The collision energy of the soft-landed species, determined by the potential difference between the CQ DC offset and the surface, was in a range of 30−35 eV/charge translating to an ion kinetic energy of ∼90 eV for POM^{3-} and 60 eV for POM^{2-}. Kinetic energydependent studies were conducted by biasing the surface with an appropriate negative potential. The ion current on the surface was measured with a picoammeter (model 9103, RBD Instruments, Bend, OR) and remained steady throughout the deposition. Typical ion currents of mass-selected POM anions were as follows: 500−600 pA for 90 eV deposition of POM^{3-}, 160−240 pA for 25 and 30 eV depositions of POM^{3-}, and 150−180 pA for 60 eV deposition of POM^{2-}.

Charge buildup on the SAM surfaces occurs during ion deposition and was described in detail previously for soft landing of cations.[24,30] A large potential buildup on the surface may repulse/deflect the ions approaching the surface, effectively stopping the deposition. We calculate a maximum negative

dx.doi.org/10.1021/jp505050m | J. Phys. Chem. C 2014, 118, 27611−27622

potential buildup of ~6 V due to charge accumulation by depositing 2×10^{13} triply charged anions onto an area with a diameter of 10 mm, film thickness of 1 nm, and a dielectric constant of the SAM of 2.3.[24,30] This potential buildup is not large enough to block ion beams with kinetic energy values in the range of 25−90 eV used in this study.

In Situ Infrared Reflection Absorption Spectroscopy. As described in previous publications,[66,67] IRRAS experiments were performed using a Bruker Vertex 70 Fourier transform infrared (FTIR) spectrometer (Bruker Optics, Billerica, MA) equipped with a liquid-nitrogen-cooled mercury−cadmium−telluride (MCT) detector. The IR beam exiting the spectrometer was deflected with a flat gold-coated mirror and focused on the SAM-Au surface in the deposition chamber using a gold-coated parabolic mirror with a diameter of 50 mm and a focal length of 400 mm. A mid-infrared ZnSe wire grid polarizer was placed between the SAM-Au surface and the parabolic mirror to ensure that the incident IR beam was *p*-polarized with respect to the surface. The reflected light was focused on the externally mounted MCT detector using two additional parabolic mirrors. The angle of incidence was 80° with respect to surface normal. IR spectra were obtained by acquiring 1500 scans (~6 min) with 4 cm^{-1} resolution at 10 min intervals during the deposition. The IR beam path was constantly purged with N_2 gas during the experiments to minimize atmospheric contributions to the signal.

Electrochemical Measurements. CV measurements were performed using a Princeton Applied Research (PAR) potentiostat (VersaStat4, Princeton, NJ) in a three-electrode configuration with Ag/AgCl as a reference electrode in saturated KCl, a platinum wire as the counter electrode, and the prepared POM-SAM-Au surface as the working electrode. The working electrode was placed in a modified plate material evaluation cell (catalog no. 011951, ALS, Japan). The liquid electrolyte consisted of 0.5 M H_2SO_4 in deionized water obtained from an Ultrapure Milli-Q system (resistivity: 18.2 MΩ-cm at 25 °C). The electrolyte solution was deoxygenated by purging with argon gas before and during the measurements. A minimum of 20 cycles were acquired for each of the surfaces at scan rates 20, 50, and 100 mVs^{-1} in the potential range of 0.5 to −0.1 V. All experiments were conducted at room temperature.

Theoretical Methods. Optimization of the structures of $PMo_{12}O_{40}^{3-}$ (POM^{3-}), $PMo_{12}O_{40}^{2-}$ (POM^{2-}), $PMo_{12}O_{40}^{-}$ (POM^{-}), $PMo_{12}O_{40}$ (POM^{0}), and $HPMo_{12}O_{40}^{2-}$ ($HPOM^{2-}$) as well as the calculation of their vibrational frequencies were performed using density functional theory (DFT). The calculations employed the B3LYP hybrid exchange-correlation functional. The 6-311G** basis set[70,71] was used for the H, O, and P atoms, and the Stuttgart relativistic effective core potential (ECP) and atomic basis set[72−74] were used for the Mo atoms. All geometry optimization and frequency calculations were performed using the NWChem quantum chemistry code.[75] The structures of the singly protonated POM^{3-} ($HPOM^{2-}$) were obtained by attaching a proton to a terminal (O_t) or bridging oxygen site (O_{b1}, O_{b2}) of a geometry-optimized POM^{3-} and reoptimizing to find the lowest energy structure.

RESULTS AND DISCUSSION

Identifying Charge Retention by Soft Landed POM Anions Using Vibrational Spectroscopy. We examined charge retention and redox properties of POM^{3-} and POM^{2-} deposited onto three SAM surfaces, which have distinctly different chemical and electronic properties. The calculated lowest energy structure of the isolated Keggin anion ($PMo_{12}O_{40}^{3-}$) and bond designations along with schematic structures of the FSAM, HSAM, and NH_3^+SAM surfaces are shown in Figure 1. The FSAM surface is known to be

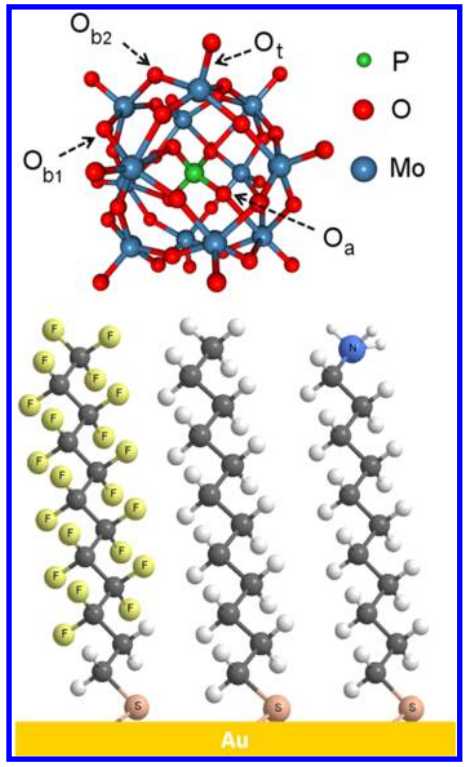

Figure 1. Calculated lowest energy structure of Keggin phosphomolybdate ($PMo_{12}O_{40}^{3-}$). Four types of oxygen sites are identified by O_a (internal), O_t (terminal), O_{b1}, and O_{b2} (bridging). The molecular structures of the FSAM (left), HSAM (center), and NH_3^+SAM (right) surfaces are also shown schematically.

hydrophobic,[76] relatively inert, and prone to retain the charge of deposited cations.[28,29,61] Similar to the FSAM, the HSAM surface is also relatively unreactive, but has little or no barrier for tunneling of electrons from the underlying gold surface,[31] resulting in efficient charge reduction of both protonated and native cations deposited on top.[22,30,33,37] The NH_3^+SAM is a hydrophilic surface[65] with readily available protons when prepared under acidic conditions. Anions such as POM^{3-} have been shown to immobilize strongly on the NH_3^+SAM due to electrostatic attraction with the positively charged terminal amine groups.[62,77]

Previously, we investigated charge retention of soft-landed cations on SAM surfaces using in situ time-of-flight secondary ion mass spectrometry (TOF-SIMS), observing intact precursor cations.[29,30,33,35,78] In this study, TOF-SIMS analysis of the soft landed POM anions on SAM surfaces resulted in the complete fragmentation of deposited POMs into $(MoO_3)_n$ (n = 1, 2, 3, 4...) subunits (Figure S1 of Supporting Information) induced by the high-energy sputtering and ionization processes. As a result, it was not possible to distinguish between different charge states of soft-landed POMs using TOF-SIMS. Therefore, we developed an alternative approach for the in situ analysis of the charge state and structure of deposited anions using IRRAS combined with DFT calculations.

dx.doi.org/10.1021/jp505050m | J. Phys. Chem. C 2014, 118, 27611−27622

The IRRAS spectra obtained following soft landing of POM^{3-} on the three different SAM surfaces are presented in Figure 2. Each spectrum was obtained by soft landing ~2 × 10^{13} POM^{3-} ions on the respective SAM surfaces. Because the anions are mass-selected before deposition, our experiments reveal the vibrational features of isolated monodisperse POMs without the contribution of contaminants such as counter cations or solvent molecules, which are present when POM species are adsorbed onto surfaces from solution.

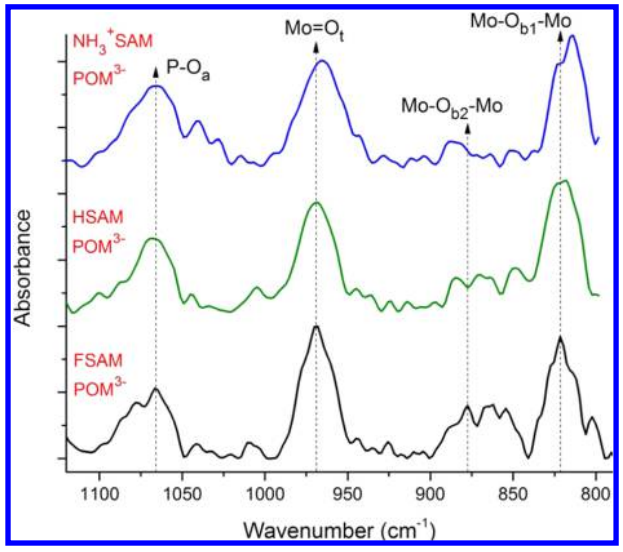

Figure 2. Experimental IRRAS spectra obtained following deposition of 2 × 10^{13} POM^{3-} ions on FSAM, HSAM, and NH_3^+SAM surfaces. The dashed lines represent the key vibrational features of the POMs including P−O_a (1060−1080 cm^{-1}), Mo═O_t (950−970 cm^{-1}), Mo−O_{b2}−Mo (860−880 cm^{-1}), and Mo−O_{b1}−Mo (805−820 cm^{-1}). Peak positions are provided in Table S1 of the Supporting Information.

Although the major vibrational features of POM^{3-} have been well-characterized previously both experimentally[79−81] and theoretically,[55,56,82,83] to the best of our knowledge, the vibrational spectra of isolated POM anions deposited onto well-defined surfaces have not been reported thus far. The frequencies reported in the literature for the asymmetric P−O stretch (P−O_a in Figure 2) are within the range of 1060−1080 cm^{-1}, while the Mo═O terminal stretch (Mo═O_t) appears between 950 and 970 cm^{-1}. The two types of bridging oxygen bands[56,84] contribute to vibrational features at ~860−880 cm^{-1} (Mo−O_{b2}−Mo) and ~805−820 cm^{-1} (Mo−O_{b1}−Mo), respectively. The distinction between these two bridging oxygen centers is that the O_{b1} atoms bind to a Mo atom that is directly connected to the internal PO_4 group of the POM, while the O_{b2} atoms only bind to Mo atoms that do not form a bond with the PO_4 core. Also, the Mo−O_{b1}−Mo bridging band appears at a lower wavenumber range in comparison with the Mo−O_{b2}−Mo band. This weakening of the O_{b1} bridging band may be attributed to the fact that the Mo atoms that contribute to the Mo−O_{b1}−Mo band have to share electron density with the oxygen atoms of the internal PO_4 group.

The simulated infrared absorbance spectra based on DFT calculations of isolated POM^{3-}, POM^{2-}, POM^{-}, and neutral POM molecules are shown in Figure 3. For comparison, the experimental spectrum of POM^{3-} deposited onto FSAM is also provided. In the IRRAS spectrum of POM^{3-} soft-landed onto FSAM, the P−O_a, Mo═O_t, Mo−O_{b2}−Mo, and Mo−O_{b1}−Mo

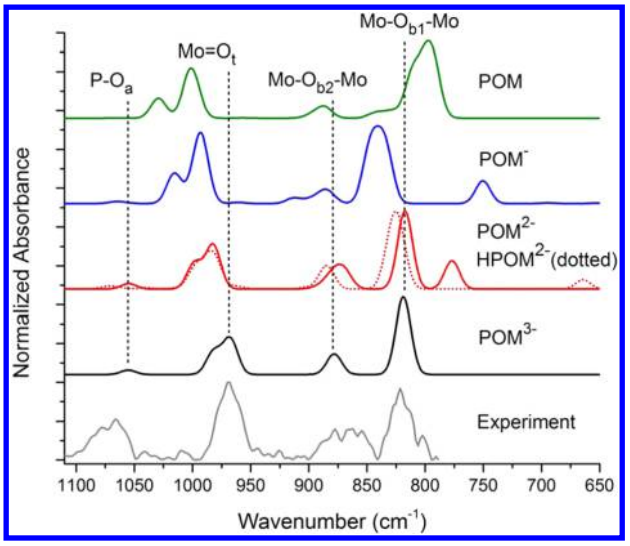

Figure 3. Simulated infrared absorbance spectra of isolated POM^{3-}, POM^{2-}, POM^{-}, POM^{0}, and $HPOM^{2-}$ molecules obtained by DFT calculations compared with the experimental spectrum of POM^{3-} deposited on FSAM (shown in gray). In the simulated spectra, the changes to the vibrational features depending on the charge state of the POM may be visualized with aid of the black dotted lines. The black dotted lines are intended to aid the visualization of the direction of peak shifts and changes in peak shapes of the charge reduced POMs relative to POM^{3-}.

vibrations were observed at 1066, 968, 877, and 821 cm^{-1}, respectively, in good agreement with the values reported in the literature. The calculated changes in band positions for different charge states are useful for understanding how charge reduction affects the vibrational features of the POM. Because POM species may also experience charge reduction by protonation, the vibrational spectrum of $HPOM^{2-}$ was calculated. Although the bridging oxygen atoms are preferred as initial protonation sites,[83,85] we calculated the vibrational spectra of $HPOM^{2-}$ by singly protonating a terminal (O_t) site as well as the two bridging sites (O_{b2},O_{b1}) of the geometrically optimized POM^{3-} and subsequently reoptimizing the geometry for the lowest energy structure. Both calculations showed similar vibrational features, notably the pronounced appearance of a lower wavenumber feature related to the Mo═O_t (~960 cm^{-1}) band (Tables S2−S4 in the Supporting Information) and a blue shift of the bridging bands. The key changes in the calculated peak positions and shapes for the major vibrational features of each charge state as well as the protonated POM are summarized in Table S5 of the Supporting Information.

To further understand the behavior of supported POMs in different ionic charge states, we examined the experimental vibrational features of mass-selected POM^{2-} soft-landed onto both FSAM and NH_3^+SAM surfaces. POM^{2-} was produced by ESI from the same solution used to electrospray POM^{3-}, although, under similar instrument settings, the POM^{2-} abundance was at least three times lower than that of POM^{3-} (mass spectrum of POM^{2-} and POM^{3-} produced by ESI is shown in Figure S2 of the Supporting Information). Similar to the POM^{3-} experiments, ~2 × 10^{13} ions of mass-selected POM^{2-} were deposited. The vibrational features of the Mo═O_t (~960 cm^{-1}) and Mo−O_{b2}−Mo (~880 cm^{-1}) bands of POM^{2-} and POM^{3-} are compared in Figure 4. On the FSAM (Figure 4a), a distinct change in the shape and position of the Mo═O_t band is observed for the two different charge states of

dx.doi.org/10.1021/jp505050m | J. Phys. Chem. C 2014, 118, 27611−27622

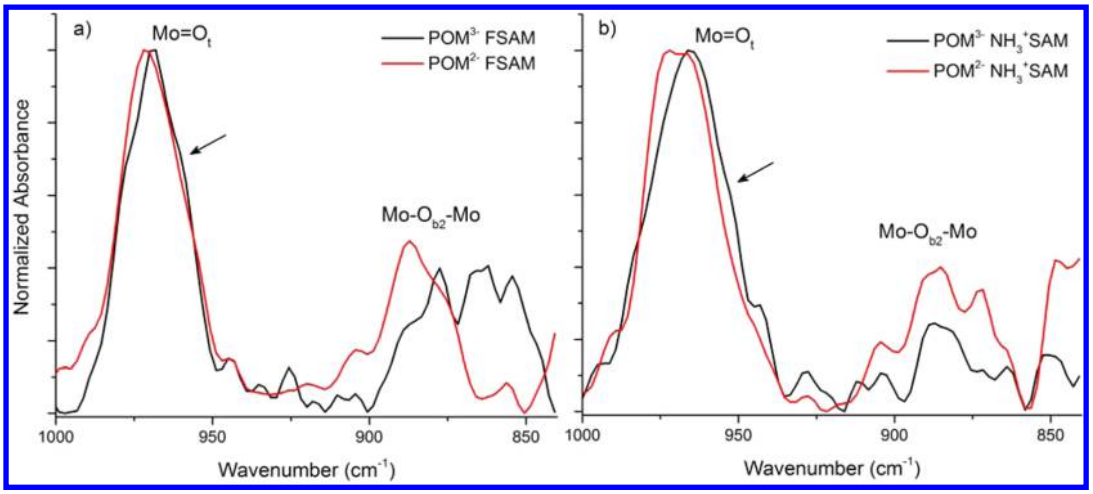

Figure 4. Comparison of the experimental IRRAS spectra of POM^{2-} (red) and POM^{3-} (black) soft-landed on (a) FSAM and (b) NH_3^+SAM surfaces. These spectra have been baseline corrected, and the intensities are normalized. The 1000−840 cm^{-1} range was chosen to highlight the differences in peak positions and shapes for the Mo═O_t (~960 cm^{-1}) and Mo−O_{b2}−Mo (~880 cm^{-1}) bands.

the POM. Specifically, for the soft-landed POM^{2-}, we observe a slight blue shift of the Mo═O_t band (Figure 4a: red), and the absence of the low-energy shoulder is indicated by the arrow in Figure 4a. Similarly, the Mo═O_t band for POM^{2-} deposited on the NH_3^+SAM surface shows a shift to higher wavenumbers and the absence of the low-energy shoulder (indicated by the arrow in Figure 4b). Incidentally, this is the first instance where POM^{2-} was selectively isolated from solution for soft landing, emphasizing the powerful capabilities of preparative mass spectrometry.

Terminal Mo═O_t Bands. The IRRAS results shown in Figure 2 reveal that the Mo═O_t band of POM^{3-} on FSAM has better resolved sub-bands compared with POM^{3-} on the HSAM and NH_3^+SAM surfaces. The Mo═O_t band on the HSAM has the same position and width as that on the FSAM with less defined subfeatures. The same band on the NH_3^+SAM is red-shifted and broader. Because DFT calculations reveal that the terminal Mo═O_t band (~960−980 cm^{-1}) undergoes systematic changes in both position and shape as a function of the POM charge state (Figure 3), we will primarily focus on this band for understanding charge retention by soft-landed POM anions. According to calculations, the position of this band shifts to higher wavenumbers with reduced charge. The Mo═O_t band for isolated POM^{3-} is calculated to be at 969 cm^{-1}, while it appears at 983, 993, and 1001 cm^{-1} for POM^{2-}, POM^-, and POM^0, respectively. The physical origin of this shift is attributed to the terminal O_t atoms moving closer to the POM cage structure with reduced POM charge, resulting in stronger Mo═O_t bonds. This peak is composed of two bands and the separations between these bands also increase with decreasing charge state (Figure 3). In the experimental IRRAS spectra (Figures 2 and 4), we observe a lower wavenumber shoulder at ~960 cm^{-1} and a peak at ~970 cm^{-1}. Because the DFT calculations show a difference of ~10 cm^{-1} between the terminal band positions of 3- and 2- POMs, we assign the shoulder at ~960 cm^{-1} as a signature of POM^{3-} and the peak at ~970 cm^{-1} as a signature of POM^{2-}. The Mo═O_t peak positions for POM^{2-} and $HPOM^{2-}$ are calculated to be similar, with the $HPOM^{2-}$ peak being slightly broader due to a lower wavenumber shoulder (shown in Figure 3 and highlighted in Tables S2−S4 in Supporting Information).

The experimentally observed vibrational features of the Mo═O_t band of POM^{3-} soft-landed on an FSAM are compared with the features of POM^{3-} deposited on an HSAM and NH_3^+SAM in Figure 5. For FSAM and HSAM, the

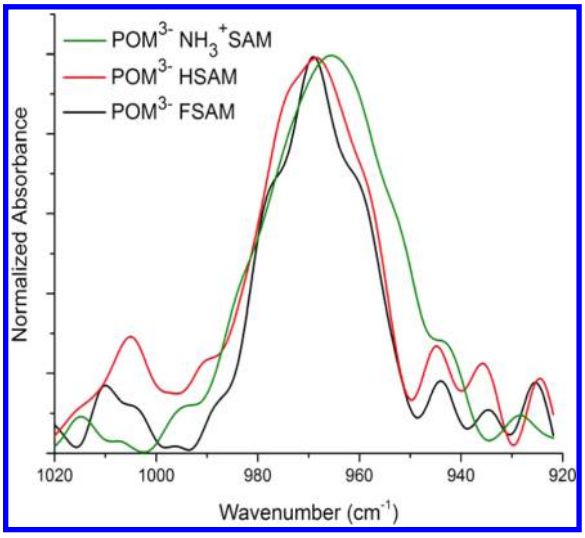

Figure 5. Overlap of the Mo═O_t bands observed experimentally after depositing 2 × 10^{13} POM^{3-} on FSAM, HSAM, and NH_3^+SAM.

Mo═O_t bands are similar in width, while a significantly broader Mo═O_t band is observed on NH_3^+SAM. To compare the extent of charge retention by soft-landed POM^{3-} on FSAM and HSAM, we extracted time-dependent intensities of POM^{3-} (~960 cm^{-1}) and POM^{2-} (~970 cm^{-1}) during deposition and plotted the ratio of intensity values of POM^{3-}/POM^{2-} as a function of time in Figure 6. The intensities of individual features corresponding to POM^{3-} and POM^{2-} were obtained by fitting the experimental Mo═O_t bands acquired during the deposition process with a sum of Gaussians. Both the absolute values and the time dependence of the POM^{3-}/POM^{2-} intensity ratios obtained on the FSAM and HSAM surfaces are similar. This analysis indicates that similar proportions of charged POM anions are retained on both the FSAM and HSAM. This was unexpected given the large differences in electron-transfer properties of these two surfaces previously

dx.doi.org/10.1021/jp505050m | J. Phys. Chem. C 2014, 118, 27611−27622

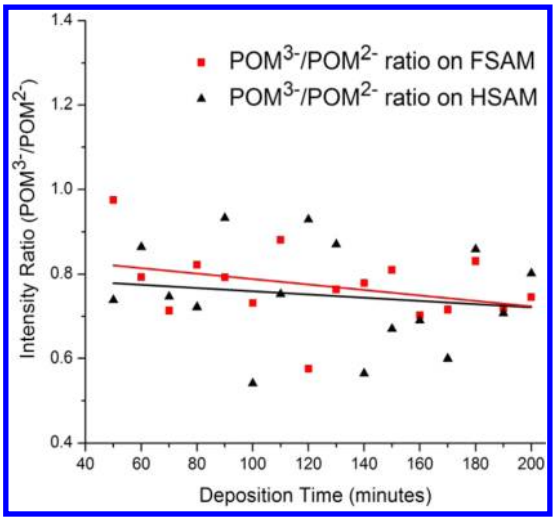

Figure 6. Time dependence of the IR intensity ratio of POM^{3-}/POM^{2-} during the deposition obtained by fitting the shape of the Mo═O_t band with a sum of Gaussians. Estimated ions soft landed: 4 × 10^{12} (at 50 min) to 2 × 10^{13} (at 200 min).

observed,[31,32] with the FSAM typically exhibiting better charge retention of soft-landed cations than the HSAM.[24,28,29] On the FSAM, the highly electronegative fluorine atoms withdraw electron density from the alkyl chains while simultaneously inducing an interface dipole at the FSAM−Au interface.[31,32] For cations, this combined effect was found to introduce a barrier for electron transfer from the underlying metal surface through the FSAM layer to the cations resting on top,[29,61] and a number of studies have demonstrated efficient retention of charge by soft-landed cations[20,28,30,66] on FSAMs. On the other hand, the fact that the HSAM has little or no barrier for electron transfer through the alkyl chain[31,86] allows for efficient charge reduction of soft-landed cations on this surface.[29,30,37] Because the charge retention of anions on the HSAM observed in the present study is in contrast with the almost complete neutralization previously reported for cations soft-landed onto identical surfaces, it is reasonable to assume that charge retention by POM anions is not determined by the electron-transfer properties of the SAM surface. Instead, we propose that the electron binding energy of the anions plays an important role in determining the extent of charge retention.

The gas-phase adiabatic electron binding energy of POM^{3-} has been previously measured by Waters et al.[87] to be 1.99 eV. The soft-landed POM anions would first need to overcome this energy barrier to undergo charge reduction by electron detachment. This is a substantial barrier that may prevent charge reduction of thermalized anions on the HSAM surface following deposition. No distinct charge reduction is observed over time for anions that are thermalized on the surface following soft landing, as shown by the negligible deviation of the POM^{3-}/POM^{2-} ratio for both surfaces during the course of the deposition (Figure 6). Because there is evidence of partial charge reduction of soft-landed anions and no indication of charge reduction after thermalization, we hypothesize that charge reduction of the deposited anions occurs at the time of collision with the surface. This is similar to the instantaneous charge loss observed for soft-landed cations discussed in previous studies.[30,33] It was suggested that, for the cations, the kinetic energy of the ions during collision could promote charge loss. It is then reasonable to expect that the kinetic energy of POM anions at the time of collision provides sufficient energy to overcome the electron binding energy necessary for electron detachment, prompting the subsequent charge reduction of a fraction of the POMs.

To determine the effect of kinetic energy of the projectile ions on the extent of charge retention, we examined the vibrational spectra of POM^{3-} ions deposited onto FSAMs at 25, 30, and 90 eV. These experiments were conducted by applying a negative bias to the substrate, effectively slowing down the approaching anions prior to deposition. The results obtained following deposition of ∼1 × 10^{13} anions at these three kinetic energies are shown in Figure 7, while detailed time-dependent

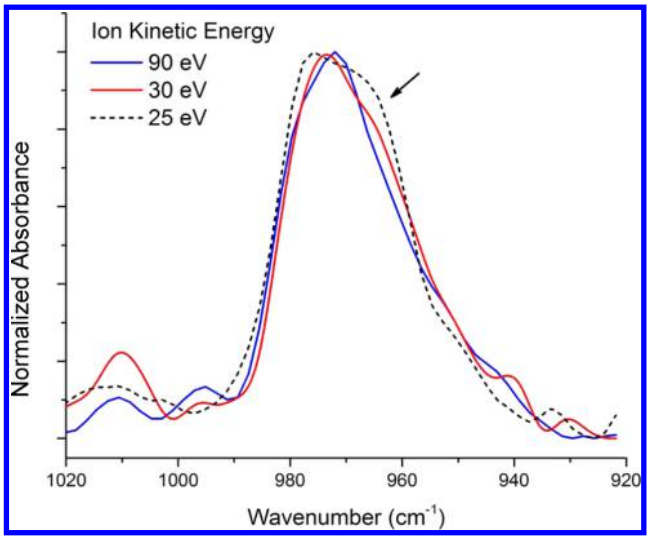

Figure 7. Effect of ion kinetic energy on the terminal Mo═O_t band of soft-landed POMs. The arrow points to the increasing intensity of the lower wavenumber shoulder observed when lowering the kinetic energy of the ions. This increase in intensity is attributed to an increase in POM^{3-} anions on the SAM surface at lower deposition energies.

data are presented in Figures S4−S6 of the Supporting Information. As shown in Figure 7, the lower wavenumber shoulder of the Mo═O_t band (∼964 cm^{-1}) increases in intensity with decreasing ion kinetic energy. As previously discussed, DFT calculations predict the Mo═O_t band to shift to higher wavenumbers with decreasing charge state of the POM (Figure 3). The observed increase in intensity of the lower wavenumber shoulder is consistent with better charge retention by ions deposited at lower kinetic energy (Figure 7). This observation provides further support for the charge-reduction mechanism for anions proposed in this study, in which electron detachment from the anion promoted by kinetic energy at the time of collision, is the rate-limiting step.

In addition to charge reduction, POM anions may undergo dissociative landing at higher collision energies. Dissociation may result in deposition of the $(MoO_3)_n$ (n = 1, 2, 3...) fragments observed in our TOF-SIMS analysis (Figure S1 in the Supporting Information) or larger anions observed in collision-induced dissociation (CID) studies of phosphotungstates.[88] Both $(MoO_3)_n$ fragments and the larger anions have vibrational features in the range of the terminal and bridging bands of the intact POM.[89,90] To the best of our knowledge, dissociation thresholds for the POM anions examined in this study are not known. Dissociation thresholds for smaller transition metal oxide clusters are in the range of 3−6 eV.[17,91] It is likely that threshold energies for larger POM anions are

dx.doi.org/10.1021/jp505050m | J. Phys. Chem. C 2014, 118, 27611−27622

lower than 3 eV. However, because of the size of POMs examined in this study, their dissociation may be accompanied by a substantial kinetic shift.[92] The kinetic shift was estimated using Rice−Ramsperger−Kassel−Marcus (RRKM) calculations of the unimolecular rate for dissociation of POM assuming a conservative low dissociation threshold of 2 eV. Rapid internal excitation of the ion in collision with the surface and subsequent efficient dissipation of the excess internal energy of the ion to the surface occur on a time scale of picoseconds.[93] It follows that both dissociative deposition and charge reduction induced by collision are characterized by rate constants in excess of 10^{10} s^{-1}. RRKM calculations indicate the corresponding kinetic shift is >15 eV. Of note, this is the lower estimate obtained using a fairly low threshold energy of 2 eV. The average kinetic-to-internal energy transfer in collisions of polyatomic ions with FSAM surfaces is ∼20%.[94] Therefore, an average internal energy of 5, 6, and 18 eV is deposited into POM during soft landing at 25, 30, and 90 eV, respectively. On the basis of the results of RRKM calculations, it is reasonable to assume that fragmentation may occur in a fraction of 90 eV collisions, while the majority of POM anions soft-landed at 25 and 30 eV would not undergo fragmentation. In support of these estimates, when examining the four major vibrational bands observed in the 1100−800 cm^{-1} range for the POM^{3-} deposition (Figure S7 in Supporting Information), there are no obvious kinetic-energy-dependent effects on the relative intensities or positions of each peak. This leads us to infer that even at 90 eV fragmentation of POMs is minimal.

Bridging Mo−O−Mo and Internal P−O_a Bands. According to DFT calculations, the two bridging (O_b) bands and the internal P−O_a band of POM do not show a consistent trend with charge state similar to the terminal Mo═O_t bands. The Mo−O_{b2}−Mo band position is calculated to first shift to lower wavenumber for POM^{2-} and then to higher wavenumber for POM^{-} and neutral POM. The Mo−O_{b1}−Mo band also does not show a systematic red or blue shift with reducing charge. Instead, this band is calculated to be similar for POM^{3-} and POM^{2-}, while showing a blue shift and red shift for POM^{-} and POM^{0}, respectively. The calculated frequency for the P−O_a band trends $POM^{3-} \approx POM^{2-} < POM^{-} < POM^{0}$ with the $HPOM^{2-}$ showing a shift to higher wavenumber with reducing charge (Table S5 of the Supporting Information).

The experimental Mo−O_{b2}−Mo band (∼860−880 cm^{-1}) obtained by in situ IRRAS shows broad features on all three surfaces, and the relative intensities were noted to decrease in the order FSAM > HSAM > NH_3^+SAM. The Mo−O_{b2}−Mo band for POM^{2-} soft-landed on FSAM shows a blue shift (Figure 4a: red) relative to the same band of the POM^{3-} on FSAM. On the NH_3^+SAM surface, this band for POM^{2-} has relatively higher intensity compared with the POM^{3-} spectrum. This observed blue shift of the bridging Mo−O_{b2}−Mo band may indicate an additional IR signature of POM anions with reduced charge. The experimental Mo−O_{b1}−Mo and P−O_a bands of POM^{3-} and POM^{2-} soft-landed on FSAM appear at similar positions, in agreement with the DFT calculations for these two charge states (Table S1 and S5 in the Supporting Information). Unlike the terminal Mo═O_t band, the vibrational signatures due to the two bridging bands, Mo−O_{b1}−Mo and Mo−O_{b2}−Mo, do not show systematic trends. As discussed previously, the terminal Mo═O_t bond gets shorter with reduced POM charge. Therefore, the O_{b1} and O_{b2} atoms may need to readjust their positions to compensate for Coulombic repulsion due to the closer terminal O_t atoms as well as the internal O_a atoms.

Analysis of the observed vibrational bands indicates that the surfaces prepared by soft landing POM^{3-} on the FSAMs may contain POMs with an overall higher charge distribution (mainly POM^{3-} and POM^{2-}), while the surfaces prepared by soft landing POM^{2-} are composd of mostly POM^{2-} with contributions from the singly charged and neutral POMs. A list of all peak positions (in the 1100−800 cm^{-1} region) for the four major bands of the soft-landed POM^{3-} and POM^{2-} on each of the SAM surfaces is provided in Table S1 of the Supporting Information.

Protonation. For POM anions deposited onto NH_3^+SAM surfaces, both electron detachment and proton attachment from the surface may contribute to charge reduction. As a result, the NH_3^+SAM surface likely retains a combination of charge-reduced POM and protonated POM anions. DFT calculations revealed vibrational features of the singly protonated POM ($HPOM^{2-}$), as shown in Figure 3 and Table S5 in the Supporting Information. Relatively minor but distinguishable differences exist between the calculated vibrational spectra of $HPOM^{2-}$ and POM^{2-} (Figure 3). The calculated IR spectrum of $HPOM^{2-}$ shows band broadening due to the lower wavenumber feature of the Mo═O_t band (∼960 cm^{-1}) and a blue shift of the bridging oxygen bands. Also, the experimental vibrational features of POMs soft-landed on NH_3^+SAM are broader than on either the FSAM and HSAM surfaces (Figure 5). We attribute this observed broadening to be signatures of the protonation products formed by POM−NH_3^+SAM interactions.

Previous calculations performed by Janik et al.[83] for an isolated phosphotunsgate ion suggested electron donation by the terminal (Mo═O_t) double bond to accommodate the formation of O−H bonds in protonated POMs. For $PMo_{12}O_{40}^{3-}$, we calculate a similar result for the Mo═O_t band (∼960 cm^{-1}). The donation of electron density weakens the Mo═O_t bond, which results in a lower wavenumber feature observed at ∼960 cm^{-1} in Figure 3 ($HPOM^{2-}$: red dotted line). Our calculations show this IR feature regardless of whether the first proton was added to a terminal (O_t) or a bridging (O_{b2} and O_{b1}) location of the bare POM^{3-} (highlighted modes in Table S2−S4 of the Supporting Information), in good agreement with the prior work on protonated phosphotungstates.[83]

In summary, by comparing our in situ IRRAS spectra with DFT calculations, we were able to identify vibrational features of soft-landed POM anions in different charge states. We also attributed the unexpected charge retention of anions on HSAMs to the large electron binding energy of the POM anions while demonstrating that the kinetic energy of the soft-landed ions can be used to tune the extent of instantaneous charge loss during collision. For protonated surfaces, an additional pathway for charge reduction involves the formation of protonated POMs on the surface.

Redox Activity of Soft Landed POM^{3-} and POM^{2-}. The POM anions deposited on NH_3^+SAMs are strongly bound compared with the other surfaces. This became evident during postdeposition electrochemical testing in solution, where the POM-NH_3^+SAM surfaces showed persistent redox activity for repeated CV experiments, whereas on the HSAM and FSAM surfaces, redox activity was observed in the first few CV scans but rapidly disappeared in subsequent CV testing, thereby indicating that the POMs were washed away from the surface.

dx.doi.org/10.1021/jp505050m | J. Phys. Chem. C 2014, 118, 27611−27622

This strong immobilization on NH_3^+SAM is attributed to the electrostatic attraction between the POM anions and the positively charged (NH_3^+) surface groups.[62,77,95] Stable immobilization of the POM anions on the NH_3^+SAMs allowed us to compare the redox properties of surfaces prepared by soft-landing POMs in different charge states (3− vs 2−). In addition, we acquired CV data for POMs adsorbed onto NH_3^+SAMs from 100 μM solutions of $H_3Mo_{12}O_{40}$ (H_3POM) and $Na_3Mo_{12}O_{40}$ (Na_3POM) in methanol for comparison with the data obtained for soft-landed POMs. The electrochemical results obtained at a scan rate of 20 mVs^{-1} are shown in Figure 8, while CV data obtained at all scan rates (20, 50, and 100 mVs^{-1}) are presented in Figure S3 of the Supporting Information. Table S6 of the Supporting Information lists the redox potentials and currents, the peak current ratio for each redox couple [(I(anodic)/I(cathodic)], midpotentials, as well as the peak separations for each redox couple.

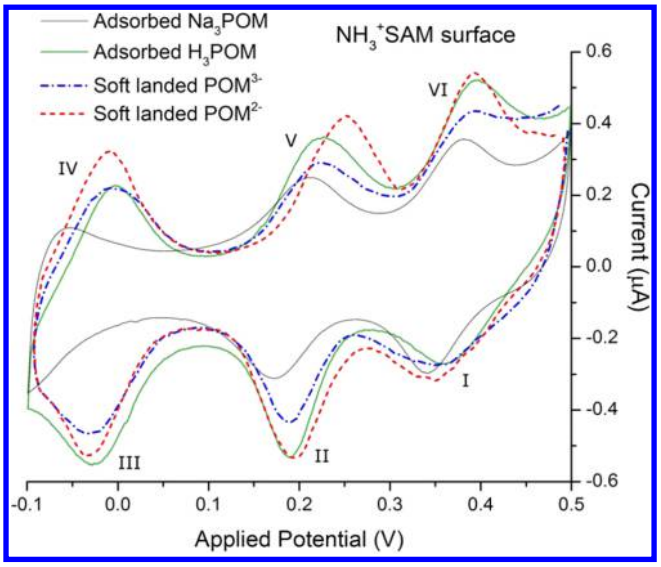

Figure 8. Cyclic voltammograms of POM^{3-} (blue dashed dotted) and POM^{2-} (red dashed) soft-landed on NH_3^+SAM surfaces compared with Na_3POM (gray) and H_3POM (green) adsorbed from solutions. All scans were obtained at a rate of 20 mVs^{-1} after 20 cycles. All measurements are made with reference to a Ag/AgCl electrode in saturated KCl.

The redox couples observed in the CV of H_3POM (Figure 8: green) and Na_3POM (Figure 8: gray) adsorbed from solution are consistent with the data reported previously in the literature.[96−99] In an acidic electrolyte, the redox activity of phosphomolybdates is known to involve two proton and two electron processes typically described as follows[97,98]

$$\mathbf{POM^{3-}} + 2H^+ + 2e^- \rightarrow H_2POM^{3-} \quad \text{(I)}$$

$$H_2POM^{3-} + 2H^+ + 2e^- \rightarrow H_4POM^{3-} \quad \text{(II)}$$

$$H_4POM^{3-} + 2H^+ + 2e^- \rightarrow H_6POM^{3-} \quad \text{(III)}$$

$$H_6POM^{3-} - 2H^+ - 2e^- \rightarrow H_4POM^{3-} \quad \text{(IV)}$$

$$H_4POM^{3-} - 2H^+ - 2e^- \rightarrow H_2POM^{3-} \quad \text{(V)}$$

$$H_2POM^{3-} - 2H^+ - 2e^- \rightarrow \mathbf{POM^{3-}} \quad \text{(VI)}$$

The ability to precisely control the charge state of deposited ions is important for understanding its effect on redox properties. In this study, we used CV to compare, for the first time, the electrochemical activity of soft-landed POM anions with a sample prepared by absorption of POMs from solution. Remarkably, the measured redox activity of 2×10^{13} POM^{3-} anions soft-landed on the NH_3^+SAM surface (Figure 8: blue) was found to be analogous to that of POM adsorbed from the H_3POM solution (Figure 8: green), indicating that both surfaces have equivalent electrochemical activity. However, it should be emphasized that surface modification by ion soft landing uses a much smaller amount of material than POM deposition from solution and contains only the anions of interest. We first compared the redox properties of POM anions adsorbed from H_3POM and Na_3POM solutions onto NH_3^+SAM surfaces. There is an observed shift of reduction potentials toward more negative values for POMs adsorbed onto NH_3^+SAMs from the Na_3POM solution, with respect to H_3POM (Figure 8: gray, green). Similar decreases in reduction potentials have been observed previously and attributed to the presence of less electronegative counter cations, in this case, Na^+.[100] This observation highlights the unique potential of selective substrate preparation through ion soft landing for studying the intrinsic properties of ions on surfaces in the absence of counter cations or anions that can exert an unwanted influence on properties.

One substantial difference between the two surfaces prepared by soft landing of specific POM charge states is the increased potential gap for the II/V redox couple of the POM^{2-} deposition (57 mV) relative to POM^{3-} (33 mV). This increase in potential gap is consistent with the presence of an additional barrier for this step of the redox process on the surface prepared by soft landing POM^{2-}, which influences the electron-transfer rate (Figure 8: step V).[97] The formation of an intermediate with a higher binding energy for protons or electrons may contribute to the increased potential gap observed for this redox couple. This finding suggests that surfaces prepared with different initial charge-state distributions of the same species may have distinctly different electrochemical properties. We propose that ion soft landing may be used for tuning the electrochemical properties of surfaces by controlling the charge state of deposited ions. A recent study by Vilá-Nadal et al.[101] suggested that carefully designed Wells-Dawson POM anions may be used as alternative charge storage centers in molecular memory storage devices. It has been demonstrated that both the charge and redox activity of POM anions have a significant effect on their charge storage capacity in a multi-bit memory cell. Such potential technological advances further illustrate the value of fundamental studies using the highly-controlled deposition conditions we have discussed herein.

Control over the size, composition, and ionic charge state of deposited material distinguishes ion soft landing from traditional surface modification approaches. The ability to select the charge state enables a detailed understanding of its effect on redox properties and makes it possible to gain unprecedented insights into how the structure and reactivity of supported molecules evolve as a function of charge. The results presented in this study demonstrate that by utilizing soft landing to prepare well-defined surfaces composed of different charge-state distributions of POMs, hitherto unobserved structural and electrochemical phenomena may be studied. Having the ability to selectively deposit specific charge states of electronically,

physically, chemically, and electrochemically interesting metal oxides as well as gain control over the distribution of ionic charge states on surfaces will facilitate ongoing investigations into fundamental structure−function relationships that are critical to the directed design of improved materials for a variety of potential technological applications.

CONCLUSIONS

This study examined the charge retention and redox properties of soft-landed multiply charged anions by combining in situ IRRAS, DFT calculations, and ex situ CV. The vibrational spectra and redox activity of two separate charge states of phosphomolybdate anions, POM^{3-} and POM^{2-}, supported on surfaces were investigated. The ion−surface interactions were examined by comparing the vibrational spectra of POMs on FSAM, HSAM, and NH_3^+SAM surfaces. In contrast with the behavior previously observed for cations, the FSAM and HSAM surfaces retained similar charge distributions of soft-landed multiply charged anions. Therefore, the charge-retention properties of anions are proposed to be dictated primarily by the electron-binding energy of the anions and not the electronic properties of the surface, as is the case for cations.

The electrochemical response of the surfaces prepared by soft-landing POM^{3-} and POM^{2-} was comparable to H_3POM adsorbed from solution onto NH_3^+SAMs, demonstrating the ability to study redox properties of minute amounts of POM deposited by ion soft landing using conventional macroscopic electrochemical techniques. Distinctive differences in the CVs were identified for one redox couple when comparing the soft-landed POM^{3-} and POM^{2-} on NH_3^+SAMs, highlighting the possibility of preparing surfaces with tunable redox behavior using very small quantities of charge-selected material. Such a distinction would not have been observed on surfaces prepared using any other technique. We have demonstrated that ion soft landing may be utilized to selectively prepare substrates with different charge-state distributions of anionic POMs, thereby offering a powerful approach for tuning the chemical and electronic properties of surfaces.

ASSOCIATED CONTENT

Supporting Information

Negative-mode TOF-SIMS analysis of surfaces prepared by soft-landing POM^{3-}, mass spectra of major POM anions produced by ESI, DFT results of protonated POM ($HPMo_{12}O_{40}^{2-}$), evolution of the vibrational spectra during kinetic energy-dependent experiments, and CV data. This material is available free of charge via the Internet at http://pubs.acs.org.

AUTHOR INFORMATION

Corresponding Author

*E-mail: Julia.Laskin@pnnl.gov.

Present Address

[†]School of Mechanical and Materials Engineering, Washington State University, Pullman, Washington 99164-2920, United States

Notes

The authors declare no competing financial interest.

ACKNOWLEDGMENTS

This work was supported by the U.S. Department of Energy (DOE), Office of Basic Energy Sciences, Division of Chemical Sciences, Geosciences & Biosciences. This work was performed using EMSL, a national scientific user facility sponsored by the DOE's Office of Biological and Environmental Research and located at PNNL. PNNL is operated by Battelle for the U.S. DOE.

REFERENCES

(1) Yoon, B.; Häkkinen, H.; Landman, U.; Wörz, A. S.; Antonietti, J.-M.; Abbet, S.; Judai, K.; Heiz, U. Charging Effects on Bonding and Catalyzed Oxidation of CO on Au_8 Clusters on MgO. *Science* **2005**, *307*, 403−407.

(2) Sterrer, M.; Risse, T.; Martinez Pozzoni, U.; Giordano, L.; Heyde, M.; Rust, H.-P.; Pacchioni, G.; Freund, H.-J. Control of the Charge State of Metal Atoms on Thin MgO Films. *Phys. Rev. Lett.* **2007**, *98*, 096107.

(3) Leoni, T.; Guillermet, O.; Walch, H.; Langlais, V.; Scheuermann, A.; Bonvoisin, J.; Gauthier, S. Controlling the Charge State of a Single Redox Molecular Switch. *Phys. Rev. Lett.* **2011**, *106*, 216103.

(4) Repp, J.; Meyer, G.; Olsson, F. E.; Persson, M. Controlling the Charge State of Individual Gold Adatoms. *Science* **2004**, *305*, 493−495.

(5) Fu, Y.-S.; Zhang, T.; Ji, S.-H.; Chen, X.; Ma, X.-C.; Jia, J.-F.; Xue, Q.-K. Identifying Charge States of Molecules with Spin-Flip Spectroscopy. *Phys. Rev. Lett.* **2009**, *103*, 257202.

(6) Simic-Milosevic, V.; Heyde, M.; Nilius, N.; König, T.; Rust, H. P.; Sterrer, M.; Risse, T.; Freund, H. J.; Giordano, L.; Pacchioni, G. Au Dimers on Thin MgO(001) Films: Flat and Charged or Upright and Neutral? *J. Am. Chem. Soc.* **2008**, *130*, 7814−7815.

(7) Gross, L.; Mohn, F.; Liljeroth, P.; Repp, J.; Giessibl, F. J.; Meyer, G. Measuring the Charge State of an Adatom with Noncontact Atomic Force Microscopy. *Science* **2009**, *324*, 1428−1431.

(8) Fernández-Torrente, I.; Kreikemeyer-Lorenzo, D.; Stróżecka, A.; Franke, K. J.; Pascual, J. I. Gating the Charge State of Single Molecules by Local Electric Fields. *Phys. Rev. Lett.* **2012**, *108*, 036801.

(9) Yan, S.; Ding, Z.; Xie, N.; Gong, H.; Sun, Q.; Guo, Y.; Shan, X.; Meng, S.; Lu, X. Turning On and Off the Rotational Oscillation of a Single Porphine Molecule by Molecular Charge State. *ACS Nano* **2012**, *6*, 4132−4136.

(10) Pacchioni, G.; Giordano, L.; Baistrocchi, M. Charging of Metal Atoms on Ultrathin MgO/Mo(100) Films. *Phys. Rev. Lett.* **2005**, *94*, 226104.

(11) Pacchioni, G. Electronic Interactions and Charge Transfers of Metal Atoms and Clusters on Oxide Surfaces. *Phys. Chem. Chem. Phys.* **2013**, *15*, 1737−1757.

(12) Lee, J.-S.; Kim, Y.-M.; Kwon, J.-H.; Shin, H.; Sohn, B.-H.; Lee, J. Tunable Memory Characteristics of Nanostructured, Nonvolatile Charge Trap Memory Devices Based on a Binary Mixture of Metal Nanoparticles as a Charge Trapping Layer. *Adv. Mater.* **2009**, *21*, 178−183.

(13) Kim, S.-J.; Lee, J.-S. Flexible Organic Transistor Memory Devices. *Nano Lett.* **2010**, *10*, 2884−2890.

(14) Lightstone, J. M.; Patterson, M. J.; Liu, P.; Lofaro, J. C., Jr.; White, M. G. Characterization and Reactivity of the $Mo_4S_6^+$ Cluster Deposited on Au(111). *J. Phys. Chem. C* **2008**, *112*, 11495−11506.

(15) Molina, L. M.; Hammer, B. The Activity of the Tetrahedral Au_{20} Cluster: Charging and Impurity Effects. *J. Catal.* **2005**, *233*, 399−404.

(16) Johnson, G. E.; Mitrić, R.; Nössler, M.; Tyo, E. C.; Bonačić-Koutecký, V.; Castleman, A. W. Influence of Charge State on Catalytic Oxidation Reactions at Metal Oxide Clusters Containing Radical Oxygen Centers. *J. Am. Chem. Soc.* **2009**, *131*, 5460−5470.

(17) Zemski, K. A.; Justes, D. R.; Castleman, A. W. Studies of Metal Oxide Clusters: Elucidating Reactive Sites Responsible for the Activity of Transition Metal Oxide Catalysts. *J. Phys. Chem. B* **2002**, *106*, 6136−6148.

(18) Lang, S. M.; Bernhardt, T. M. Gas Phase Metal Cluster Model Systems for Heterogeneous Catalysis. *Phys. Chem. Chem. Phys.* **2012**, *14*, 9255−9269.

(19) Zhao, Y.-X.; Wu, X.-N.; Ma, J.-B.; He, S.-G.; Ding, X.-L. Characterization and Reactivity of Oxygen-Centred Radicals over

Transition Metal Oxide Clusters. *Phys. Chem. Chem. Phys.* **2011**, *13*, 1925−1938.
(20) Gologan, B.; Green, J. R.; Alvarez, J.; Laskin, J.; Graham Cooks, R. Ion/Surface Reactions and Ion Soft-Landing. *Phys. Chem. Chem. Phys.* **2005**, *7*, 1490−1500.
(21) Grill, V.; Shen, J.; Evans, C.; Cooks, R. G. Collisions of Ions with Surfaces at Chemically Relevant Energies: Instrumentation and Phenomena. *Rev. Sci. Instrum.* **2001**, *72*, 3149−3179.
(22) Johnson, G. E.; Hu, Q.; Laskin, J. Soft Landing of Complex Molecules on Surfaces. *Annu. Rev. Anal. Chem.* **2011**, *4*, 83−104.
(23) Verbeck, G. F.; Hoffman, W.; Walton, B. Soft-Landing Preparative Mass Spectrometry. *Analyst* **2012**, 4393−4407.
(24) Laskin, J.; Wang, P.; Hadjar, O. Soft-landing of Peptide Ions onto Self-Assembled Monolayer Surfaces: An Overview. *Phys. Chem. Chem. Phys.* **2008**, *10*, 1079−1090.
(25) Cyriac, J.; Pradeep, T.; Kang, H.; Souda, R.; Cooks, R. G. Low-Energy Ionic Collisions at Molecular Solids. *Chem. Rev.* **2012**, *112*, 5356−5411.
(26) Rao, C. N. R.; Kulkarni, G. U.; Thomas, P. J.; Edwards, P. P. Metal Nanoparticles and their Assemblies. *Chem. Soc. Rev.* **2000**, *29*, 27−35.
(27) Ammam, M. Polyoxometalates: Formation, Structures, Principal Properties, Main Deposition Methods and Application in Sensing. *J. Mater. Chem. A* **2013**, *1*, 6291−6312.
(28) Miller, S. A.; Luo, H.; Pachuta, S. J.; Cooks, R. G. Soft-Landing of Polyatomic Ions at Fluorinated Self-Assembled Monolayer Surfaces. *Science* **1997**, *275*, 1447−1450.
(29) Johnson, G. E.; Priest, T.; Laskin, J. Charge Retention by Gold Clusters on Surfaces Prepared Using Soft Landing of Mass Selected Ions. *ACS Nano* **2011**, *6*, 573−582.
(30) Johnson, G. E.; Priest, T.; Laskin, J. Coverage-Dependent Charge Reduction of Cationic Gold Clusters on Surfaces Prepared Using Soft Landing of Mass-Selected Ions. *J. Phys. Chem. C* **2012**, *116*, 24977−24986.
(31) Pflaum, J.; Bracco, G.; Schreiber, F.; Colorado, R., Jr.; Shmakova, O. E.; Lee, T. R.; Scoles, G.; Kahn, A. Structure and Electronic Properties of CH_3- and CF_3-terminated Alkanethiol Monolayers on Au(111): A Scanning Tunneling Microscopy, Surface X-ray and Helium Scattering Study. *Surf. Sci.* **2002**, *498*, 89−104.
(32) Alloway, D. M.; Hofmann, M.; Smith, D. L.; Gruhn, N. E.; Graham, A. L.; Colorado, R.; Wysocki, V. H.; Lee, T. R.; Lee, P. A.; Armstrong, N. R. Interface Dipoles Arising from Self-Assembled Monolayers on Gold: UV−Photoemission Studies of Alkanethiols and Partially Fluorinated Alkanethiols. *J. Phys. Chem. B* **2003**, *107*, 11690−11699.
(33) Hadjar, O.; Futrell, J. H.; Laskin, J. First Observation of Charge Reduction and Desorption Kinetics of Multiply Protonated Peptides Soft Landed onto Self-Assembled Monolayer Surfaces. *J. Phys. Chem. C* **2007**, *111*, 18220−18225.
(34) Wang, P.; Hadjar, O.; Gassman, P. L.; Laskin, J. Reactive Landing of Peptide Ions on Self-Assembled Monolayer Surfaces: An Alternative Approach for Covalent Immobilization of Peptides on Surfaces. *Phys. Chem. Chem. Phys.* **2008**, *10*, 1512−1522.
(35) Alvarez, J.; Cooks, R. G.; Barlow, S. E.; Gaspar, D. J.; Futrell, J. H.; Laskin, J. Preparation and in Situ Characterization of Surfaces Using Soft Landing in a Fourier Transform Ion Cyclotron Resonance Mass Spectrometer. *Anal. Chem.* **2005**, *77*, 3452−3460.
(36) Volný, M.; Elam, W. T.; Ratner, B. D.; Tureček, F. Preparative Soft and Reactive Landing of Gas-Phase Ions on Plasma-Treated Metal Surfaces. *Anal. Chem.* **2005**, *77*, 4846−4853.
(37) Hadjar, O.; Wang, P.; Futrell, J. H.; Laskin, J. Effect of the Surface on Charge Reduction and Desorption Kinetics of Soft Landed Peptide Ions. *J. Am. Soc. Mass Spectrom.* **2009**, *20*, 901−906.
(38) Ouyang, Z.; Takáts, Z.; Blake, T. A.; Gologan, B.; Guymon, A. J.; Wiseman, J. M.; Oliver, J. C.; Davisson, V. J.; Cooks, R. G. Preparing Protein Microarrays by Soft-Landing of Mass-Selected Ions. *Science* **2003**, *301*, 1351−1354.
(39) Nagaoka, S.; Okada, E.; Doi, S.; Mitsui, M.; Nakajima, A. Trapping of V(benzene)$_2$ Sandwich Clusters in a n-Alkanethiol Self-Assembled Monolayer Matrix. *Eur. Phys. J. D* **2005**, *34*, 239−242.
(40) Volný, M.; Sadílek, M.; Jackson, K. E.; Diener, M.; Elam, W. T.; Tureček, F. Matrix-Free Laser Desorption/Ionization of Ions Landed on Plasma-Treated Metal Surfaces. *J. Mass Spectrom.* **2008**, *43*, 1265−1273.
(41) Hamann, C.; Woltmann, R.; Hong, I. P.; Hauptmann, N.; Karan, S.; Berndt, R. Ultrahigh Vacuum Deposition of Organic Molecules by Electrospray Ionization. *Rev. Sci. Instrum.* **2011**, *82*, 033903−033903−6.
(42) Papaconstantinou, E.; Pope, M. T. Heteropoly Blues. III. Preparation and Stabilities of Reduced 18-Molybdodiphosphates. *Inorg. Chem.* **1967**, *6*, 1152−1155.
(43) Katsoulis, D. E. A Survey of Applications of Polyoxometalates. *Chem. Rev.* **1998**, *98*, 359−388.
(44) Long, D.-L.; Tsunashima, R.; Cronin, L. Polyoxometalates: Building Blocks for Functional Nanoscale Systems. *Angew. Chem., Int. Ed.* **2010**, *49*, 1736−1758.
(45) Song, Y.-F.; Tsunashima, R. Recent Advances on Polyoxometalate-based Molecular and Composite Materials. *Chem. Soc. Rev.* **2012**, *41*, 7384−7402.
(46) Yamase, T. Photo- and Electrochromism of Polyoxometalates and Related Materials. *Chem. Rev.* **1998**, *98*, 307−326.
(47) Wang, H.; Hamanaka, S.; Nishimoto, Y.; Irle, S.; Yokoyama, T.; Yoshikawa, H.; Awaga, K. In Operando X-ray Absorption Fine Structure Studies of Polyoxometalate Molecular Cluster Batteries: Polyoxometalates as Electron Sponges. *J. Am. Chem. Soc.* **2012**, *134*, 4918−4924.
(48) Mizuno, N.; Misono, M. Heteropolyacid Catalysts. *Curr. Opin. Solid State Mater. Sci.* **1997**, *2*, 84−89.
(49) Douglas, T.; Young, M. Host-Guest Encapsulation of Materials by Assembled Virus Protein Cages. *Nature* **1998**, *393*, 152−155.
(50) Jing, B.; Hutin, M.; Connor, E.; Cronin, L.; Zhu, Y. Polyoxometalate Macroion Induced Phase and Morphology Instability of Lipid Membrane. *Chem. Sci.* **2013**, *4*, 3818−3826.
(51) Hakouk, K.; Oms, O.; Dolbecq, A.; El Moll, H.; Marrot, J.; Evain, M.; Molton, F.; Duboc, C.; Deniard, P.; Jobic, S.; Mialane, P.; Dessapt, R. Sulfonium Polyoxometalates: A New Class of Solid-State Photochromic Hybrid Organic−Inorganic Materials. *Inorg. Chem.* **2013**, *52*, 555−557.
(52) Glezos, N.; Argitis, P.; Velessiotis, D.; Diakoumakos, C. D. Tunneling Transport in Polyoxometalate Based Composite Materials. *Appl. Phys. Lett.* **2003**, *83*, 488−490.
(53) Douvas, A. M.; Makarona, E.; Glezos, N.; Argitis, P.; Mielczarski, J. A.; Mielczarski, E. Polyoxometalate-Based Layered Structures for Charge Transport Control in Molecular Devices. *ACS Nano* **2008**, *2*, 733−742.
(54) Rocchiccioli-Deltcheff, C.; Fournier, M.; Franck, R.; Thouvenot, R. Vibrational Investigations of Polyoxometalates. 2. Evidence for Anion-Anion Interactions in Molybdenum(VI) and Tungsten(VI) Compounds Related to the Keggin Structure. *Inorg. Chem.* **1983**, *22*, 207−216.
(55) López, X.; Maestre, J. M.; Bo, C.; Poblet, J.-M. Electronic Properties of Polyoxometalates: A DFT Study of α/β-$[XM_{12}O_{40}]^{n-}$ Relative Stability (M = W, Mo and X a Main Group Element). *J. Am. Chem. Soc.* **2001**, *123*, 9571−9576.
(56) Bridgeman, A. J. Computational Study of the Vibrational Spectra of α- and β-Keggin Polyoxometalates. *Chem.—Eur. J.* **2004**, *10*, 2935−2941.
(57) Teague, C. M.; Li, X.; Biggin, M. E.; Lee, L.; Kim, J.; Gewirth, A. A. Vibrational Spectroscopy of a Keggin Polyoxometalate on Metal Electrode Surfaces. *J. Phys. Chem. B* **2004**, *108*, 1974−1985.
(58) Thiel, J.; Molina, P. I.; Symes, M. D.; Cronin, L. Insights into the Self-Assembly Mechanism of the Modular Polyoxometalate "Keggin-Net" Family of Framework Materials and their Electronic Properties. *Cryst. Growth Des.* **2011**, *12*, 902−908.
(59) Proust, A.; Matt, B.; Villanneau, R.; Guillemot, G.; Gouzerh, P.; Izzet, G. Functionalization and Post-Functionalization: A Step

Towards Polyoxometalate-based Materials. *Chem. Soc. Rev.* **2012**, *41*, 7605−7622.
(60) Miras, H. N.; Yan, J.; Long, D.-L.; Cronin, L. Engineering Polyoxometalates with Emergent Properties. *Chem. Soc. Rev.* **2012**, *41*, 7403−7430.
(61) Laskin, J.; Wang, P.; Hadjar, O.; Futrell, J. H.; Alvarez, J.; Cooks, R. G. Charge Retention by Peptide Ions Soft-Landed onto Self-Assembled Monolayer Surfaces. *Int. J. Mass Spectrom.* **2007**, *265*, 237−243.
(62) Wang, S.; Du, D. Preparation and Electrochemical Properties of Keggin-Type Phosphomolybdic Anions in Electrostaticly Linked l-Cysteine Self-Assembled Monolayers. *Sens. Actuators, B* **2003**, *94*, 282−289.
(63) Ron, H.; Matlis, S.; Rubinstein, I. Self-Assembled Monolayers on Oxidized Metals. 2. Gold Surface Oxidative Pretreatment, Monolayer Properties, and Depression Formation. *Langmuir* **1998**, *14*, 1116−1121.
(64) Fukushima, H.; Seki, S.; Nishikawa, T.; Takiguchi, H.; Tamada, K.; Abe, K.; Colorado, R.; Graupe, M.; Shmakova, O. E.; Lee, T. R. Microstructure, Wettability, and Thermal Stability of Semifluorinated Self-Assembled Monolayers (SAMs) on Gold. *J. Phys. Chem. B* **2000**, *104*, 7417−7423.
(65) Wang, H.; Chen, S.; Li, L.; Jiang, S. Improved Method for the Preparation of Carboxylic Acid and Amine Terminated Self-Assembled Monolayers of Alkanethiolates. *Langmuir* **2005**, *21*, 2633−2636.
(66) Hu, Q.; Wang, P.; Gassman, P. L.; Laskin, J. In situ Studies of Soft- and Reactive Landing of Mass-Selected Ions Using Infrared Reflection Absorption Spectroscopy. *Anal. Chem.* **2009**, *81*, 7302−7308.
(67) Hu, Q.; Wang, P.; Laskin, J. Effect of the Surface on the Secondary Structure of Soft Landed Peptide Ions. *Phys. Chem. Chem. Phys.* **2010**, *12*, 12802−12810.
(68) Fenn, J.; Mann, M.; Meng, C.; Wong, S.; Whitehouse, C. Electrospray Ionization for Mass Spectrometry of Large Biomolecules. *Science* **1989**, *246*, 64−71.
(69) Shaffer, S. A.; Prior, D. C.; Anderson, G. A.; Udseth, H. R.; Smith, R. D. An Ion Funnel Interface for Improved Ion Focusing and Sensitivity Using Electrospray Ionization Mass Spectrometry. *Anal. Chem.* **1998**, *70*, 4111−4119.
(70) Krishnan, R.; Binkley, J. S.; Seeger, R.; Pople, J. A. Self-Consistent Molecular Orbital Methods. XX. A Basis Set for Correlated Wave Functions. *J. Chem. Phys.* **1980**, *72*, 650−654.
(71) McLean, A. D.; Chandler, G. S. Contracted Gaussian Basis Sets for Molecular Calculations. I. Second Row Atoms, Z=11−18. *J. Chem. Phys.* **1980**, *72*, 5639−5648.
(72) Bergner, A.; Dolg, M.; Küchle, W.; Stoll, H.; Preuß, H. Ab Initio Energy-Adjusted Pseudopotentials for Elements of Groups 13−17. *Mol. Phys.* **1993**, *80*, 1431−1441.
(73) Kaupp, M.; Schleyer, P. v. R.; Stoll, H.; Preuss, H. Pseudopotential Approaches to Ca, Sr, and Ba Hydrides. Why are some Alkaline Earth MX_2 Compounds Bent? *J. Chem. Phys.* **1991**, *94*, 1360−1366.
(74) Dolg, M.; Stoll, H.; Preuss, H.; Pitzer, R. M. Relativistic and Correlation Effects for Element 105 (hahnium, Ha): A Comparative Study of M and MO (M = Nb, Ta, Ha) Using Energy-Adjusted Ab Initio Pseudopotentials. *J. Phys. Chem.* **1993**, *97*, 5852−5859.
(75) Valiev, M.; Bylaska, E. J.; Govind, N.; Kowalski, K.; Straatsma, T. P.; Van Dam, H. J. J.; Wang, D.; Nieplocha, J.; Apra, E.; Windus, T. L.; de Jong, W. A. NWChem: A Comprehensive and Scalable Open-Source Solution for Large Scale Molecular Simulations. *Comput. Phys. Commun.* **2010**, *181*, 1477−1489.
(76) Patois, T.; Et Taouil, A.; Lallemand, F.; Carpentier, L.; Roizard, X.; Hihn, J.-Y.; Bondeau-Patissier, V.; Mekhalif, Z. Microtribological and Corrosion Behaviors of 1H,1H,2H,2H-perfluorodecanethiol Self-Assembled Films on Copper Surfaces. *Surf. Coat. Technol.* **2010**, *205*, 2511−2517.
(77) Cheng, L.; Niu, L.; Gong, J.; Dong, S. Electrochemical Growth and Characterization of Polyoxometalate-Containing Monolayers and Multilayers on Alkanethiol Monolayers Self-Assembled on Gold Electrodes. *Chem. Mater.* **1999**, *11*, 1465−1475.
(78) Alvarez, J.; Futrell, J. H.; Laskin, J. Soft-Landing of Peptides onto Self-Assembled Monolayer Surfaces. *J. Phys. Chem. A* **2005**, *110*, 1678−1687.
(79) Thouvenot, R.; Fournier, M.; Franck, R.; Rocchiccioli-Deltcheff, C. Vibrational Investigations of Polyoxometalates. 3. Isomerism in Molybdenum(VI) and Tungsten(VI) Compounds Related to the Keggin Structure. *Inorg. Chem.* **1984**, *23*, 598−605.
(80) Song, I. K.; Kaba, M. S.; Barteau, M. A. STM Investigation of Pyridine Interaction with Heteropoly Acid Monolayers. *J. Phys. Chem.* **1996**, *100*, 17528−17534.
(81) Gómez-Romero, P.; Lira-Cantú, M. Hybrid Organic-Inorganic Electrodes: The Molecular Material Formed Between Polypyrrole and the Phosphomolybdate Anion. *Adv. Mater.* **1997**, *9*, 144−147.
(82) Guo, Y.-R.; Pan, Q.-J.; Wei, Y.-D.; Li, Z.-H.; Li, X. Theoretical Studies on the Electronic and Spectroscopic Properties of Keggin-Structure Polyoxometalates α/β-$[XM_{12}O_{40}]^{n-}$ (X=Si, P; M=Mo, W). *J. Mol. Struct.* **2004**, *676*, 55−64.
(83) Janik, M. J.; Campbell, K. A.; Bardin, B. B.; Davis, R. J.; Neurock, M. A Computational and Experimental Study of Anhydrous Phosphotungstic Acid and its Interaction with Water Molecules. *Appl. Catal., A* **2003**, *256*, 51−68.
(84) Yan, L.; López, X.; Carbó, J. J.; Sniatynsky, R.; Duncan, D. C.; Poblet, J. M. On the Origin of Alternating Bond Distortions and the Emergence of Chirality in Polyoxometalate Anions. *J. Am. Chem. Soc.* **2008**, *130*, 8223−8233.
(85) Efremenko, I.; Neumann, R. Protonation of Phosphovanadomolybdates $H_{3+x}PV_xMo_{12-x}O_{40}$: Computational Insight Into Reactivity. *J. Phys. Chem. A* **2011**, *115*, 4811−4826.
(86) Wang, J.-g.; Selloni, A. Influence of End Group and Surface Structure on the Current−Voltage Characteristics of Alkanethiol Monolayers on Au(111). *J. Phys. Chem. A* **2007**, *111*, 12381−12385.
(87) Waters, T.; Huang, X.; Wang, X.-B.; Woo, H.-K.; O'Hair, R. A. J.; Wedd, A. G.; Wang, L.-S. Photoelectron Spectroscopy of Free Multiply Charged Keggin Anions α-$[PM_{12}O_{40}]^{3-}$ (M = Mo, W) in the Gas Phase. *J. Phys. Chem. A* **2006**, *110*, 10737−10741.
(88) Ma, M. T.; Waters, T.; Beyer, K.; Palamarczuk, R.; Richardt, P. J. S.; O'Hair, R. A. J.; Wedd, A. G. Gas-Phase Fragmentation of Polyoxotungstate Anions. *Inorg. Chem.* **2008**, *48*, 598−606.
(89) Glaser, T.; Beck, S.; Lunkenheimer, B.; Donhauser, D.; Köhn, A.; Kröger, M.; Pucci, A. Infrared Study of the MoO_3 Doping Efficiency in 4,4′-bis(N-carbazolyl)-1,1′-biphenyl (CBP). *Org. Electron.* **2013**, *14*, 575−583.
(90) Bridgeman, A. J.; Cavigliasso, G. Density Functional Study of the Vibrational Frequencies of Lindqvist Polyanions. *Chem. Phys.* **2002**, *279*, 143−159.
(91) Armentrout, P. Reactions and Thermochemisty of Small Transition Metal Cluster Ions. *Annu. Rev. Phys. Chem.* **2001**, *52*, 423−461.
(92) Lifshitz, C. Kinetic shifts. *Eur. J. Mass Spectrom.* **2002**, *8*, 85−98.
(93) Song, K.; Meroueh, O.; Hase, W. L. Dynamics of $Cr(CO)_6^+$ Collisions with Hydrogenated Surfaces. *J. Chem. Phys.* **2003**, *118*, 2893−2902.
(94) Dongré, A. R.; Somogyi, Á.; Wysocki, V. H. Surface-induced Dissociation: An Effective Tool to Probe Structure, Energetics and Fragmentation Mechanisms of Protonated Peptides. *J. Mass Spectrom.* **1996**, *31*, 339−350.
(95) Zhong, Y. L.; Ng, W.; Yang, J.-X.; Loh, K. P. Electrostatically Self-Assembled Polyoxometalates on Molecular-Dye-Functionalized Diamond. *J. Am. Chem. Soc.* **2009**, *131*, 18293−18298.
(96) Lira-Cantú, M.; Gómez-Romero, P. Electrochemical and Chemical Syntheses of the Hybrid Organic−Inorganic Electroactive Material Formed by Phosphomolybdate and Polyaniline. Application as Cation-Insertion Electrodes. *Chem. Mater.* **1998**, *10*, 698−704.
(97) Lewera, A.; Chojak, M.; Miecznikowski, K.; Kulesza, P. J. Identification and Electroanalytical Characterization of Redox Transitions in Solid-State Keggin type Phosphomolybdic Acid. *Electroanalysis* **2005**, *17*, 1471−1476.

(98) Sadakane, M.; Steckhan, E. Electrochemical Properties of Polyoxometalates as Electrocatalysts. *Chem. Rev.* **1998**, *98*, 219−238.
(99) Itabashi, E. Medium Effects on the Redox Properties of 12-Molybdophosphate and 12-Molybdosilicate. *Bull. Chem. Soc. Jpn.* **1987**, *60*, 1333−1336.
(100) Song, I. K.; Barteau, M. A. Redox Properties of Keggin-Type Heteropolyacid (HPA) Catalysts: Effect of Counter-Cation, Heteroatom, and Polyatom Substitution. *J. Mol. Catal. A: Chem.* **2004**, *212*, 229−236.
(101) Vilà-Nadal, L.; Mitchell, S. G.; Markov, S.; Busche, C.; Georgiev, V.; Asenov, A.; Cronin, L. Towards Polyoxometalate-Cluster-Based Nano-Electronics. *Chem.—Eur. J.* **2013**, *19*, 16502−16511.